CTBP1/CYP19A1/Estradiol axis together with adipose tissue impacts over prostate cancer growth associated to metabolic syndrome

Cintia Massillo[1]; Guillermo Nicolás Dalton[1]; Juliana Porretti[1]; Georgina Daniela Scalise[1]; Paula Lucia Farré[1]; Flavia Piccioni[1]; Florencia Secchiari[2]; Natalia Pascuali[3]; Colin Clyne[4]; Kevin Gardner[5]; Paola De Luca[1]; Adriana De Siervi[1,#]

[1]Laboratorio de Oncología Molecular y Nuevos Blancos Terapéuticos, Instituto de Biología y Medicina Experimental (IBYME), CONICET; Argentina.

[2]Laboratorio de Fisiopatología de la Inmunidad Innata, Instituto de Biología y Medicina Experimental (IBYME), CONICET; Argentina.

[3]Laboratorio de Estudios de la Fisiopatología del Ovario, Instituto de Biología y Medicina Experimental (IBYME), CONICET; Argentina.

[4]Cancer Drug Discovery Laboratory, Hudson Institute of Medical Research, Clayton, Victoria 3168, Australia.

[5]Department of Pathology and Cell Biology, Columbia University Medical Center, 630 W. 168th Street, New York, NY 10032. USA.

Short title: CTBP1/CYP19A1 modulates PCa growth associated to MeS.

[#]**Corresponding Author:** Adriana De Siervi, Ph.D. Laboratorio de Oncología Molecular y Nuevos Blancos Terapéuticos, Instituto de Biología y Medicina Experimental (IBYME), CONICET. Vuelta de Obligado 2490, Buenos Aires, Argentina, C1428ADN. Phone: +5411-4783-2869, ext. 206; Fax: +5411-4786-2564; E-mail: adesiervi@dna.uba.ar

Key words: CYP19A1, Prostate Cancer, CTBP1, Metabolic Syndrome, Adipose tissue.

This article has been accepted for publication and undergone full peer review but has not been through the copyediting, typesetting, pagination and proofreading process, which may lead to differences between this version and the Version of Record. Please cite this article as doi: 10.1002/ijc.31773

Abbreviations: 5´ UTR: 5´untranslated region; ACTB: β-actin; AT: adipose tissue; CCND1: Cyclin D1; CD: control diet; ChIP: chromatin immunoprecipitation; CLS: crown like structures; CTBP: C-terminal binding protein; CYP19A1: Cytochrome P450 Family 19 Subfamily A Member 1; E_2: estradiol; EP300: E1A binding protein p300; ER: estrogen receptor; FABP4: Fatty acid binding protein 4; gWAT: gonadal white adipose tissue; HBB: β-globin; H&E: hematoxylin and eosin; HFD: high fat diet; IHC: immunohistochemistry; IL6: interleukin 6; IRS: immunorreactive Score; MCP1: Monocyte chemoattractant protein 1; MeS: metabolic syndrome; mWAT: mesenteric white adipose tissue; NSG: NOD scid gamma; PCa: prostate cancer; PEI: polyethylenimine; PPARγ: Peroxisome proliferator activated Receptor Gamma; qPCR: quantitative polymerase chain reaction; RELA: RELA proto-oncogene, NF-kB subunit; RIA: radioimmunoassay; RT: retrotranscription; SF1: Steroidogenic factor-1; STAT3: Signal transducer and activator of transcription 3; TF: transcription factor; TNF-α: Tumor necrosis factor-alpha; TSS: transcriptional start site; WAT: white adipose tissue; ZEB1: Zinc finger E-box binding homeobox 1.

Conflicts of interest: The authors declare no conflicts of interest.

Novelty and impact Statements: Chronic high fat diet intake induces metabolic syndrome (MeS) and CTBP1 activity in mice. We found that CTBP1 and MeS modulated aromatase transcription which elevated estrogen concentrations in prostate tumors. In addition, MeS induced inflammation of the white adipose tissue, leading to a proinflammatory phenotype and increased serum estradiol concentrations which impacts on prostate cancer (PCa) growth. These results have yielded unique insights into the mechanisms that link PCa development and MeS.

Abstract

Metabolic syndrome (MeS) increases prostate cancer (PCa) risk and aggressiveness. C-terminal binding protein 1 (CTBP1) is a transcriptional co-repressor of tumor suppressor genes that is activated by low NAD^+/NADH ratio. Previously, our group established a MeS and PCa mice model that identified CTBP1 as a novel link associating both diseases. We found that CTBP1 controls the transcription of aromatase (*CYP19A1*), a key enzyme that converts androgens to estrogens. The aim of this work was to investigate the mechanism that explains CTBP1 as a link between MeS and PCa based on *CYP19A1* and estrogen synthesis regulation using PCa cell lines, MeS/PCa mice and adipose co-culture systems. We found that CTBP1 and E1A binding protein p300 (EP300) bind to *CYP19A1* promoter and downregulate its expression in PC3 cells. Estradiol, through the estrogen receptor beta, released CTBP1 from *CYP19A1* promoter triggering its transcription and modulating PCa cell proliferation. We generated NSG and C57BL/6J MeS mice by chronically feeding animals with high fat diet. In the NSG model, CTBP1 depleted PCa xenografts showed an increase in the *CYP19A1* expression with the subsequent increment in intratumor estradiol concentrations. Additionally, in C57BL/6J mice, MeS induces hypertrophy, hyperplasia and inflammation of the white adipose tissue, which leads to a proinflammatory phenotype and increases serum estradiol concentration. Thus, MeS increased PCa growth and *Ctbp1*, *Fabp4* and *IL-6* expression levels. These results describe, for the first time, a novel CTBP1/CYP19A1/Estradiol axis that explains, in part, the mechanism for prostate tumor growth increase by MeS.

Introduction

Prostate cancer (PCa) is still the most prevalent cancer among men and the second leading cause of cancer death worldwide[1]. There is increasing evidence showing that diet and lifestyle play a crucial role in PCa risk and progression[2–5] Metabolic syndrome (MeS) is a cluster of pathophysiological disorders that comprises, at least, three of the following factors: visceral adiposity, high triglycerides, low High Density Lipoprotein (HDL) cholesterol levels, high blood pressure and high glucose levels[6]. Recently, a meta-analysis revealed that MeS is linked to poor prognosis in PCa patients, increased tumor aggressiveness and biochemical recurrence[7].

Previously, our group identified C-terminal binding protein 1 (CTBP1) as a molecular link associating PCa and MeS. CTBP1 is a transcriptional co-repressor of tumor suppressor genes that is activated with much higher affinity by NADH (>100-fold) compared to NAD^+[8]. Hence, we developed a MeS mice model by chronically feeding animals with high fat diet (HFD), and found that CTBP1 depletion in MeS mice dramatically decreased PCa and breast cancer growth[9,10]. Moreover, we identified a new molecular mechanism linking PCa and MeS based on Chloride Channel Accessory 2 (CLCA2) repression by CTBP1 and miR-196b-5p molecules that might act as key factors in the progression and onset of this disease[11]. Additionally, we previously reported that CTBP1 depletion in androgen insensitive PCa xenografts from HFD-fed mice induced hormone biosynthesis and metabolism-related genes, including the aromatase enzyme (CYP19A1) that is involved in the estradiol synthesis by conversion from testosterone[9].

CYP19A1 expression deregulation plays an important role in breast and endometrial cancer[12]. It was reported that estrogens induce tumors in several organs[13]. Although there is a growing body of evidence demonstrating that estrogens have effects in the progression of prostatic disease, the expression levels of *CYP19A1* and the role of estrogens in PCa remains controversial[14,15]. The dual role of estrogen, favorable and unfavorable, appears to be mediated trough an opposite action between the estrogen receptors ER-α and ER-β. The activation of ER-α leads to aberrant proliferation, inflammation and the development of premalignant lesions, while in contrast, the activation of ER-β mediates the antiproliferative, anti-inflammatory and, potentially, anticarcinogenic effects of estrogen[14]. Thus, it is important to investigate the synthesis and regulation of estrogen production, mediated by aromatase, in the prostate and the subsequent effects on prostate disease[15]. Human *CYP19A1* is encoded by a single copy of the *CYP19A1* gene, localized at chromosome 15q21.2[16]. The human *CYP19A1* gene is expressed in a tissue- and cell type-specific manner, and the complex expression and regulation of *CYP19A1* gene is achieved through the use of multiple exons that encode the 5´UTR region[17].

Visceral adiposity is one of the main aspects of MeS. Adipose tissue (AT) can be classified in brown adipose tissue (BAT) and subcutaneous and visceral white adipose tissue (WAT). Epidemiological studies correlated visceral adiposity with an increased risk of developing certain types of cancer, including colorectal, breast and endometrial[18]. WAT is an active endocrine organ secreting local and systemic hormones (leptin and adiponectin), cytokines (TNF-α and interleukin-6), growth factors (insulin-like growth factor [IGF-1],

insulin-like growth factor-binding protein [IGFBPs] and transforming growth factor [TGF-β])[18]. In men, WAT is the main site of endogenous estrogen synthesis from androgens by the aromatase enzyme located in adipocytes[19]. Adiposity deposit caused by MeS is associated to an increase in aromatase activity and in free circulating estrogen levels, and a decrease in free testosterone levels[20]. Thus, estradiol could be responsible for more aggressive prostate tumors[20].

The aim of this work was to investigate the mechanism that explains CTBP1 as a link between MeS and PCa based on aromatase and estrogen synthesis regulation. We found that CTBP1 and EP300 (E1A binding protein p300) bound directly to *CYP19A1* promoter and downregulated its expression in PCa cells. In turn, estradiol through ER-β, released CTBP1 from *CYP19A1* promoter, induced its transcription and modulated PCa cell proliferation. Moreover, we developed a NSG (NOD Scid gamma) and C57BL/6J MeS mice model by chronically feeding animals with HFD. We observed that CTBP1-depleted PCa xenografts in NSG mice showed an increase in the *CYP19A1* expression, with the consequent increment in intratumor estradiol concentrations. Additionally, MeS induced hypertrophy, hyperplasia and inflammation of WAT, which leads to a proinflammatory phenotype, serum estradiol concentration increase and PCa growth in C57BL/6J mice. Altogether, this study describes for the first time a novel *CTBP1*/*CYP19A1*/estradiol axis that provides an important link for MeS and PCa.

MATERIALS AND METHODS

Cell culture, transfections and treatments

PC3 (ATCC: CRL-1435), 22Rv1 (ATCC: CRL-2505), LNCaP (ATCC: CRL-1740), C4-2[21] cell lines and its stable derivatives were grown in RPMI-1640 (Invitrogen) supplemented with 10% of fetal bovine serum (FBS) and antibiotics in a 5% CO_2 humidified atmosphere at 37°C. These cell lines were recently validated at MDA Cancer Center (Texas, USA). PC3.shCTBP1 and its control (PC3.pGIPZ) stable cell lines were previously described[9].

TRAMP-C1 cell line (ATCC: CRL-2730) was grown in DMEM medium (GIBCO) supplemented with 10 % of FBS and antibiotics and 250 UI/µl human recombinant insulin.

PC3 cells were exposed for 48 or 96 h to estradiol (10 nM, 1 and 10 µM) or ethanol as vehicle in phenol red-free RPMI-1640 medium (GIBCO) supplemented with 10% charcoaled FBS.

PC3.pcDNA3 and pcDNA3.CTBP1 cells were generated by transient transfection using 6 µg of plasmid and polyethylenimine methodology (PEI - PolySciences INC) with PEI:DNA ratio 2:1.

Plasmids

CTBP1 plasmid and its control (pcDNA3) were previously described[10]. pGL3 plasmids with different lengths of the I.4 and PII *CYP19A1* promoter were previously described[22,23]. ZEB1 (Zinc finger E-box binding homeobox 1), EP300, E2F1 (E2F transcription factor 1) and RELA (RELA proto-oncogene, NF-kB subunit) plasmids were previously reported[24–27]. STAT3 (Signal transducer and activator of transcription 3), ER-β, ER-α and SF1 (Steroidogenic

factor-1) plasmids were kindly provided by Dr. James Darnell (Rockefeller University, United States), Dr. Christopher K. Glass (University of California, United States), Dr. Rodolfo Rey (CEDIE, Argentina) and Dr. Ken-ichirou Morohashi (Kyushu University, Japan), respectively.

Luciferase reporter assay.

PC3 cells were transfected in 12-well plates in triplicate using PEI and 1 µg of each plasmid. After 48 h of transfection, luciferase activity was determined by Luciferase Assay system (Promega) according to the manufacturer's instructions using a GloMax® 96 Microplate Luminometer (Promega). Data were normalized to total protein (determined by Bradford assay) and control.

For estradiol treatment, PC3 cells were transfected with the indicated plasmids and grown in RPMI without phenol red supplemented with charcoaled 10% FBS. After 24 h, cells were exposed to estradiol (1 and 10 µM) or vehicle for 48 h, and luciferase activity was determined as describe above.

RNA isolation, cDNA synthesis and qPCR (RT-qPCR)

Total RNA from cells, tumor xenograft, tumor allografts or gWAT was isolated using TriReagent (Molecular Research Center). cDNA synthesis was performed using 2 µg of RNA and RevertAid First Strand kit (Thermo Scientific). Real time PCR (qPCR) was performed using TAQ Pegasus (Productos Bio-Lógicos, Argentina) in a CFX96 Touch™ Real-Time PCR Detection System (Bio-Rad). Data was normalized to β-*actin* (*ACTB*) and control. Primer sequences are shown in Table S1.

Chromatin immunoprecipitation (ChIP)

PC3 cells were exposed to estradiol (1 or 10 µM) or vehicle by 96 h and fixed in 1% formaldehyde for 10 min on ice, quenched with 125 mM glycine for 15 min on ice, and washed twice in PBS containing PMSF (0.5 mM) and NaF (375 µM). Cell pellets ($7.5x10^6$ cells) were thawed on ice, resuspended in 0.5 mL of lyses buffer [50 mM Tris-HCl (pH 7.4), 1% SDS] with 1 x protease inhibitor mix (Sigma-Aldrich), and sonicated for 10 min (30 s ''on'' and 30 s ''off'') at high power using a Bioruptor® II Sonicator. This yields DNA fragments from 200–500 bp in length, with the bulk of the chromatin at 300 bp. Chromatin was immunoprecipitated from $2x10^6$ cells (130 µl of the sonicate) by using specific antibodies: 4 µg for CTBP1 (Santa Cruz Biotechnology Inc.), 2 µg for EP300[26] or 0.5 µg for non-specific Gal4 antibody (Santa Cruz Biotechnologies) with recombinant protein G beads (Invitrogen) preblocked with BSA (2 mg/mL) and DNAss (2 mg/ml) (Invitrogen). The beads were washed with 1 mL of ice-cold high-salt IP buffer [500 mM NaCl, 50 mM Tris-HCl (pH 7.4), 5 mM EDTA (pH 8.0), 0.5% Nonidet P-40, and 1% Triton X-100] once and three times with 1 mL of low-salt IP buffer [50 mM NaCl, 50 mM Tris-HCl (pH 7.4), 5 mM EDTA (pH 8.0), 0.5% Nonidet P-40, and 1% Triton X-100] (400 g, 2–3 min) and rinsed with 1ml of TE buffer [10 mM Tris-HCl (pH 8.0), 1 mM EDTA] . Then, 300 µL of buffer TE was added to the washed bead pellet, briefly vortexed, and reverse cross-linked with 0.2 mg/mL Proteinase K (Invitrogen) and 0.5 % SDS at 65 °C 16h. Samples were centrifuged (400 g, 3 min, 4°C) and ChIP-DNA in the supernatant was isolated with phenol-chloroform isoamyl, resuspended in 100 µl of H_2O and amplified by qPCR using specific primers (Table S1). Fold enrichment was calculated normalizing data to input and Gal4. The Δ-Δ Ct

method was used to calculate the fold change expression of each promoter of interest. Propagation of error was handled using standard rms methods.

Western blot (WB)

Cells were lysed and immunoblotted as previously described[28] using specific antibodies: anti-CTBP1 (Santa Cruz Biotechnology Inc.), anti-CYP19 (Santa Cruz Biotechnology Inc.) and anti-β-Actin (Cell Signaling Technology). Reactions were detected by horseradish peroxidase–conjugated secondary antibodies and enhanced chemiluminescence (Pierce) following the manufacturer's directions. Protein quantitation was performed using Image J 1.48 software (http://rsb.info.nih.gov, NIH).

Cell viability and cell cycle analysis

PCa cells were grown in media without phenol red (GIBCO) supplemented with charcoal-stripped 1 or 10% FBS. After 24 h, cells were exposed to estradiol (10 nM, 1 µM and 10 µM) or vehicle for 96 h. Cell viability was assayed by MTS (Cell-Titer-96-wells Aqueous non-Radioactive Cell-Proliferation Assay, Promega) following the manufacture instructions[28]. For cell cycle analysis, cells were fixed and stained with propidium iodide (PI), and analyzed by flow cytometry (FC) as previously described[28].

Immunosuppressed PCa xenograft and MeS murine model

Four weeks old male NSG (NOD SCID Gamma) mice (N=24), were housed under pathogen free conditions following the IBYME's animal care guidelines. Mice were randomized into 2 dietary groups and fed *ad libitum* during 16 weeks with CD (3,120 kcal/kg, 5% fat) or HFD (4,520 kcal/kg, 37% fat). Body weight was monitored once a week. After 12 weeks of

diet, mice were randomly distributed into 2 groups and injected s.c. with PC3.pGIPZ or PC3.shCTBP1 cells (4,8X10^6). Depletion of CTBP1 in PC3 cells was achieved by stably transfecting cells with a CTBP1 shRNA (sc-35122 Santa Cruz Biotechnology) vector. CTBP1 shRNA is a pool of 3 target-specific 19-25 nt siRNAs designed to knock down gene expression as previously described[9]. Tumor volume was determined three times a week and calculated as previously described[28]. Animals were sacrificed in the 16th week and tumor, liver, AT and blood samples were collected.

Non-immunodeficient PCa allografts and MeS murine model

Four weeks old male C57BL/6J mice (N=12), were housed under pathogen free conditions following the IBYME's animal care guidelines. Mice were randomized into 2 dietary groups and fed *ad libitum* during 27 weeks as described above. After 15 weeks of diet, mice were randomly distributed into 2 groups and injected s.c. with TRAMP-C1 (3X10^6) cell line. Tumor volume was determined as described above. Animals were sacrificed in the 27th week and tumor, liver, AT and blood samples were collected. Mice serum glucose, cholesterol and triglycerides levels were determined as previously described[9].

Histological and immunohistochemical (IHC) analysis

Tissue samples collected from PCa allografts and MeS mice described above were formalin-fixed and paraffin embedded (FFPE). For histological analysis, 4 µm microscopic sections were stained with hematoxylin-eosin (H&E) and examined by light microscopy. For IHC analysis of CTBP1, anti-CTBP1 antibody (1:400; 621042, BD Transduction Laboratories) was used. The procedure was completed using a streptavidin-biotin-complex method (VECTASTAIN® Universal Elite® ABC Kit, Vector Laboratories, Maravai LifeSciences)

with 3,3' diaminobenzidine (DAB) as chromogen and examined by light microscopy. IHC evaluation was performed by a pathologist without knowledge of the grouping information, using the Immunorreactive Score (IRS). The IRS gives a range of 0-12 as a product of multiplication between positive cells proportion score (0-4) and staining intensity score (0-3).

Measurement of intratumor and serum estradiol by radioimmunoassay (RIA)

Serum and intratumor estradiol levels were measured by RIA following ether extraction of steroids from 0.25 g of PC3.pGIPZ or PC3.shCTB1 tumors developed in HFD NSG mice or C57BL/6J CD or HFD mice, as previously described[29]. After tissue or serum steroid extractions, estradiol levels were determined by RIA using specific antibodies supplied by Dr. G.D. Niswender (Colorado State University, Fort Collins, CO) as previously described[30]. Under these conditions, the intra-assay and inter-assay variations were 7.2 % and 12.5% respectively. The values are expressed as pg hormone/mg of tissue for tumors and ng/ml for serum.

***Ex vivo* co-culture of gWAT with TRAMP-C1 cells**

TRAMP-C1 cells were plated in DMEM complete medium into 24-well culture plates at a density of $1.5x10^4$ cells/well. After 24 h, medium was refreshed and 150 mg of gWAT obtained from CD or HFD C57BL/6J mice were placed onto cell-culture inserts (3.0 micron pore size, high-density membrane) in M199 (SIGMA) complete medium. The experiment was conducted for a period of 48 h. Then, TRAMP-C1 cells and gWAT were collected in TriReagent for RNA isolation and RT-qPCR. As a control, TRAMP-C1 cells were incubated in

DMEM complete media without the addition of gWAT. Data were normalized to control and represent an N=6 from three different mice *per* group.

Enzyme-linked immunosorbent assay (ELISA)

Conditioned media from the co-culture were tested by competitive ELISA assay using BD OptEIA™ Set Mouse IL-6 (BD Bioscience, CA, USA) to quantify IL-6 levels following the manufacturer recommendations.

Statistical analysis

All results are given as mean and standard deviation (SD) of three independent experiments unless stated otherwise. Student t-tests or two-way ANOVA followed by Tukey test were performed. Shapiro–Wilk and Levene tests were used to assess normality and homogeneity of variances. *, $P < 0.05$; **, $P < 0.01$;***, $P < 0.001$.

Results

CTBP1 protein binds to *CYP19A1* promoter and represses its transcription.

Based in our previous finding, showing that CTBP1 repressed *CYP19A1* in PCa xenografts[9], in this work we focused on the underlying mechanism of this regulation. First, we determined *CYP19A1* gene expression in a panel of PCa cell lines, including the androgen sensitive LNCaP cells, its derived C4-2 and the androgen insensitive PC3 and 22Rv1 cells. We found that PC3 showed the highest *CYP19A1* expression (Fig. 1A). Moreover, CTBP1 overexpression decreased *CYP19A1* mRNA and protein levels in PC3 cells (Fig. 1B-C). Accordingly, *CYP19A1* mRNA was induced after CTBP1 depletion (Fig. 1D). *CTBP1* overexpression and depletion was confirmed by RT-qPCR and/or WB (Fig. 1B-D).

Several tissue-specific promoter regions were previously described for *CYP19A1*[16]. In the normal prostate, *CYP19A1* is expressed exclusively within the stroma, and is regulated via the proximal promoter PII. However, in PCa, *CYP19A1* is expressed within the epithelial tumor cells, as well as in the stromal cells, and is aberrantly regulated by promoters I.4, PII and I.3[12]. To further investigate *CYP19A1* promoter activity regulation by CTBP1, I.4 and PII reporter constructs, containing different lengths of *CYP19A1* promoter regions from the TSS, were co-transfected with CTBP1 or control (pcDNA3) plasmids into PC3 cell line. CTBP1 significantly repressed the activity of all the different *CYP19A1* promoters (Fig. 1E). Additionally, we determined that CTBP1 bound specifically to both *CYP19A1* promoter regions, I.4 and PII by ChIP (Fig. 1F). Hence, CTBP1 associates to *CYP19A1* promoter and represses its transcription in PC3 cell line.

EP300 binds to *CYP19A1* promoters and co-represses its transcription together with CTBP1.

To determine potential transcription factors (TF) that co-regulates with CTBP1 *CYP19A1* transcription, we co-transfected *CYP19A1* reporters with a panel of TFs that potentially interact with CTBP1 protein. We found that E2F1, STAT3, RELA and SF1 had no effect on *CYP19A1* promoter activity; however, EP300 repressed while ZEB1 induced its activity in PC3 cells (Fig. 2A). Furthermore, *CYP19A1* I.4 and PII promoters activity repression by CTBP1 was synergistically increased by EP300 (Fig. 2B). More importantly, using ChIP we determined that EP300 protein was physically associated to both *CYP19A1* promoters (Fig. 2C).

Although ZEB1 induced *CYP19A1* promoter activity, this activation was not influenced by CTBP1 co-transfection, suggesting that both factors act independently on *CYP19A1* transcription (Fig. S1A).

Estradiol releases CTBP1 protein from *CYP19A1* promoters triggering its transcription while EP300 remains attached.

We investigated *CYP19A1* expression regulation by estradiol in PC3 cells. In a panel of PCa cell lines, we found that PC3 cells expressed higher levels of *ER-α* and *ER*-β compared with the other cell lines (Fig. S2). Furthermore, we found that estradiol induced *CYP19A1* mRNA levels and promoter activity, which was dramatically enhanced by transfection with ER-β plasmid (Fig. 2D-E) while ER-α did not modify *CYP19A1* promoter activity (Fig. 2E). Moreover, we co-transfected PC3 cells with I.4 or PII luciferase plasmids *plus* CTBP1, ER-β or pcDNA3 vectors and, after 24 h, cells were exposed to estradiol or vehicle during 48 h, in order to detect luciferase activity. As shown in Fig. 2F, CTBP1 repressed *CYP19A1* promoter activity, even after estradiol exposure. Notably, CTBP1 attenuated *CYP19A1* promoter activity induction by ER-β and estradiol (Fig. 2F). Additionally, using ChIP we determined that CTBP1 and EP300 bound to I.4 and PII *CYP19A1* promoters, while estradiol exposure released CTBP1 protein from both promoters whilst the co-regulator EP300 remain attached (Fig. 2G).

Altogether, these results elucidate a novel function of estradiol in PCa, showing for the first time that both proteins, CTBP1 and EP300, assemble at *CYP19A1* promoter to repress

its transcription. Estradiol exposure, through ER-β, releases CTBP1 from *CYP19A1* promoter triggering its expression in androgen-insensitive PCa cells.

Estradiol modulates the viability and cell cycle progression of PCa cell lines.

Estradiol effects on PCa cell lines have been poorly investigated. Hence, we assessed the viability of a panel of PCa cell lines after exposure to estradiol. As shown in Fig. 3A, different doses of estradiol significantly increased LNCaP and C4-2 viability; however, it decreased PC3 viability, while no changes were found in 22Rv1 cell line.

In addition, we measured the percentage of LNCaP and PC3 cells in the different cell cycle phases after estradiol exposure. We found that estradiol increased 5% the percentage of S phase cells and 6% of G2/M cells in LNCaP cells (Fig. 3B). Moreover, estradiol increased 5% the G0/G1 phase PC3 cells (Fig. 3B).

Altogether, these results show that estradiol induces proliferation of androgen-sensitive cells, while it diminishes proliferation of androgen-insensitive cell lines suggesting that estradiol, ER-β, CTBP1 and EP300 constitute key regulators of *CYP19A1* expression and activity in PCa.

CTBP1 depletion dramatically increases *CYP19A1* expression and estradiol levels in xenografts from HFD fed mice.

Based in our previous results showing that CTBP1 regulated *CYP19A1* expression in PC3 xenografts developed in *nude* mice fed with HFD[9], we further investigated whether this regulation impacts over intratumor estradiol production. NSG male mice fed with HFD or

control diet (CD) during 12 weeks were inoculated with control (PC3.pGIPZ) or CTBP1-depleted (PC3.shCTBP1) PC3 stable cell lines. After 4 to 6 weeks from cell inoculation, mice were sacrificed, tumor excised and analyzed. HFD fed mice developed MeS-like disease since these animals showed dyslipidemia and liver steatosis at the end of the experiment (*data not shown*), as we previously reported for nude mice model[9]. Moreover, CTBP1 depletion significantly induced *CYP19A1* expression only in HFD group (Fig. 3C). CTBP1 depletion was confirmed in the animals by RT-qPCR (Fig. 3C). Interestingly, xenografts generated from PC3.shCTBP1 cell line showed significantly increased in intratumor estradiol levels compared to PC3.pGIPZ xenografts in HFD fed mice (Fig. 3D).

HFD increases TRAMP-C1 allograft tumor growth and serum estradiol levels while induces *Ctbp1*, *Fabp4* and *IL-6* gene expression.

Given that MeS increases serum estradiol levels, which impacts on breast tumor development[31], we investigated the effect of MeS on estrogens levels and PCa development. We generated a non-immunodeficient murine model of MeS and PCa using C57BL/6J male mice and PCa TRAMP-C1 cells. Even though, aromatase expression was undetectable in TRAMP-C1 cells by RT-qPCR before animal inoculation (*data not shown*), we found that low concentrations of estradiol significantly induced TRAMP-C1 cell viability, similarly to the result we found for human LNCaP cells (Fig. 4A). Moreover, we injected s.c. TRAMP-C1 cells into C57BL/6J male mice chronically fed with HFD or CD. Interestingly, HFD significantly increased tumor growth and serum estradiol in mice (Fig. 4B-C). It is noteworthy that C57BL/6J mice also developed MeS-like disease after

prolonged HFD intake, since they showed dyslipidemia, hyperglycemia, overweight and liver steatosis at the end of the experiment (Fig. S3A-C).

Surprisingly, molecular analysis of allograft showed that endogen *Ctbp1* mRNA levels were markedly induced by HFD without changes in *Ctbp2* gene expression (Fig. 4D). Moreover, CTBP1 IHC and IRS quantitation obtained from these allografts, demonstrated that CTBP1 protein levels was significantly higher in HFD (IRS = 5) compared to CD (IRS = 3) mice (Fig. 4E). In addition, HFD increased the expression of other genes: *Fabp4* (Fatty Acid Binding Protein 4), involved in fatty acid uptake, transport, and metabolism[32]; and the pro-inflammatory cytokine *IL6* (Interleukin 6) (Fig. 4F). No changes in *Er-α* or *Er*-β gene expression were observed in the allograft from CD compared to HFD fed mice (Fig. 4F).

HFD increases AT amount, adipocyte size and CLS in mice while induces expression of genes involved in adipogenesis and inflammation

Based on the important role of peri-prostatic AT over prostate tumor cell proliferation and migration[33], we aimed to elucidate the WAT role in PCa. First, we determined the amount of gonadal/epididymal (gWAT) and mesenteric (mWAT) AT from CD and HFD fed C57BL/6J mice. We observed a significant accumulation of both ATs in HFD fed mice compared to CD (Fig. 5A). A similar result in gWAT was found in HFD NSG mice (Fig. S4A).

Since gWAT is typically the largest and most accessible fat pad in C57BL/6J mice, we continued working with this subtype of AT. Adipocyte hypertrophy was found in gWAT from HFD compared to CD fed mice, as was determined by H&E staining (Fig. 5B).

Macrophage infiltration, determined by the presence of Crown-Like Structures (CLS), induces chronic mild inflammation, widely considered as a causative factor for insulin resistance[34]. Thus, by H&E staining we found that CLS were prevalent in gWAT from HFD fed mice compared with CD fed mice (Fig. 5C). In summary, the increase amount of AT, the adipocyte hypertrophy and the high CLS density exhibited in HFD mice, recapitulate MeS-like disease in this animal model and allow us to understand CTBP1 as a link between PCa and MeS.

In addition, we isolated RNA from HFD and CD gWAT and analyzed gene expression by RT-qPCR. We found that *Ctbp1*, *Ctbp2* and *Ccnd1* were significantly decreased in gWAT obtained from HFD fed mice (Fig. 5D). Although no significant changes were observed in *Cyp19a1* gene expression in gWAT from HFD fed mice, the dramatic increase in the amount and size of the adipocytes might suggest an increase in the concentration of estradiol which supports the serum estradiol increase in these mice (Fig. 5). *Ctbp1* and *Ccnd1* gene expression were also reduced, while no changes were observed in *Cyp19a1* expression in gWAT from HFD NSG mice (Fig. S4B). Interestingly, gWAT from HFD fed mice showed expression induction of adipogenesis and inflammation markers, including *Fabp4*, *Pparg* (Peroxisome Proliferator Activated Receptor Gamma), *Tnf-α* (Tumor Necrosis Factor α) and *Mcp1* (Monocyte Chemoattractant Protein-1) (Fig. 5E-F and Fig. S4C).

Gonadal/epididymal AT explants from HFD fed mice induced TRAMP-C1 cell proliferation and *Ctbp1*/*IL6* gene expression

To further understand the role of gWAT over prostate tumor cell proliferation and gene expression, we co-cultured gWAT from HFD fed mice or CD fed mice with TRAMP-C1 cells. Surprisingly, gWAT from HFD fed mice induced TRAMP-C1 proliferation and *Ctbp1* and *IL6* gene expression in these cells (Fig. 5G-H), similarly to the allografts developed in HFD C57BL/6J mice. Additionally, *Ctbp1*, *Fabp4* and *Pparg* expression was markedly diminished in the co-cultured gWAT from HFD fed mice (Fig. 5I). Moreover, IL-6 protein levels were increased in the conditioned medium from TRAMP-C1 cells co-cultured with gWAT from HFD mice respect to CD (Fig. 5J).

Discussion

In this report, we provide evidence of a striking linkage between *CTBP1*/*CYP19A1*/estradiol and MeS/PCa. Our goal was to understand CTBP1 role and the mechanism for PCa risk increase by MeS. Based in our previous studies, showing CTBP1 as an important link that associates PCa and MeS[9,11], we investigated *CYP19A1* regulation by CTBP1 using several PCa cell lines and mice models. We found that CTBP1 assembles with EP300 to *CYP19A1* proximal promoter region and inhibits its transcription in PCa cells. Estradiol exposure, through the ER-β, disrupts this binding and displaces CTBP1 protein from the *CYP19A1* promoter, triggering its transcription. All these data are highly relevant since there are few reports showing transcriptional regulation of *CYP19A1* expression in PCa[12,15].

Another important finding from this work was observed after estradiol treatment of a panel of PCa cell lines. Accordingly to Carruba and colleagues results[35], we found that

estradiol decreased the viability and cell cycle progression of PCa androgen insensitive cells, while it increased the viability of androgen sensitive cells.

Using immune-suppressed mice we not only confirmed the previous findings obtained in nude mice[9], but also we demonstrated that CTBP1 depleted tumors had increased concentration of intratumor estradiol, which reinforced the idea of aromatase induction in these tumors by HFD and MeS-like disease.

Other colleagues have shown that PCa cells synthesize estrogens through aromatase[15]. In this work we have shown that there is a complex transcriptional regulation of this enzyme mediated by MeS and CTBP1. We demonstrated that estrogens increased proliferation of androgen sensitive PCa cells that do not express aromatase (LNCaP and TRAMP-C1). With this scenario, new questions arise: if the prostate tumor cell responds to estrogens, but is not capable of producing it, where do the estrogens come from? How does MeS increase serum estradiol levels? Is AT playing a role in estradiol levels increase?

To answer these questions, in this work we developed a non-immunodeficient MeS mice model (C57BL/6J) whose animals were inoculated with TRAMP-C1 cells. We first confirmed that TRAMP-C1 cells used for the *in vivo* model did not express aromatase and responded to estrogens. Moreover, when we injected TRAMP-C1 cells into C57BL/6J male mice chronically fed with HFD we found significantly increased tumor growth and serum estradiol levels, supporting the idea that MeS increases serum estradiol levels impacting PCa development. Also, this model revealed that HFD fed mice showed an increased amount of AT, adipocyte hypertrophy, higher CLS density, with also adipogenesis and inflammation gene expression induction, which indicates chronic AT inflammation, an

important feature of MeS. Although no significant changes were observed in *Cyp19a1* gene expression from AT of HFD fed mice, the dramatic increase in the amount and size of the adipocytes, and the high density of CLS, might explain the increased concentration of serum estradiol in these mice. More important, we described for the first time that endogen *Ctbp1*, *Fabp4* and *IL6* were transcriptional activated by HFD in tumors. These results validated our hypothesis showing CTBP1 as a molecular link that associates MeS and PCa growth. Moreover, co-cultures determined that AT from HFD fed mice induced proliferation, *Ctbp1*, *Fabp4* and *IL6* gene expression in TRAMP-C1 cells and increased IL-6 production compared to AT from CD fed animals. Furthermore, co-culture experiments revealed that AT from HFD fed mice co-cultured with TRAMP-C1 cells showed decreased *Ctbp1* and *Fabp4* expression levels compared to CD AT. FABP4 is a low molecular weight protein that transports long-chain fatty acids released from adipocytes and macrophages and can exert its metabolic action in a paracrine or exocrine manner. It is also implicated in tumorigenesis in different cancer types, including breast, prostate and ovarian cancer, and may have an active role in the interaction between tumor and AT[32]. In fact, FABP4 is involved in lipid transfer between adipocytes and ovaric tumor cells, inducing the fatty acid oxidation pathway to fuel tumor growth[36]. In addition, in breast cancer, the expression of *FABP4* and other adipogenesis-related genes, were downregulated in AT adjacent to malignant breast tumors [37]. This process is likely due to the active lipolysis and atrophy that adipose tissue undergoes when it is in contact with cancer tissue[37]. This can be explained by the fact that FABP4 levels could be increased in peritumoral AT, but it

could be quickly released from AT to extracellular media, to transport fatty acids to adjacent tumor cells[38].

Similarly to *Wang et al*, in the co-culture of PCa cells with gWAT from CD or HFD fed mice[37], we found that HFD increased the expression of *Fabp4* in gWAT, but when AT was in contact with prostate tumor cells, there was a drastic decrease in *Fabp4* expression, compared to gWAT from CD fed mice. Altogether these data suggest that FABP4 could be more rapidly released from the adipocytes of HFD fed mice compared to CD for transport fatty acids to tumor cells. However, future experiments should be achieved to address this concern.

In summary, these results explain for the first time the molecular mechanism for PCa risk increase by MeS (*See Fig. 6 for hypothetical model*). Thus, estradiol levels increase in serum and tumors through MeS/CTBP1/CYP19A1 mechanism, which directly impacts over PCa cells proliferation. In this context, AT also contributes to stimulate proliferation. In the future, after completely elucidate the important role of AT and CTBP1/CYP19A1/estradiol axis for PCa risk, MeS patients might be advised for the elevated PCa risk to modify lifestyle habits.

Funding and acknowledgment

This research was supported by the Argentinean Agency of Science and Technology (ANPCyT PICT 2014-324; ANPCyT PICT 2015-1345). We thank the Fundación Williams (Argentina) for their support. This work was part of Ph.D thesis of Cintia Massillo supported by CONICET fellowship from Argentina.

References

1. Siegel RL, Miller KD, Jemal A. Cancer statistics, 2017. *CA Cancer J Clin* 2017;67:7–30.
2. Nunez C, Bauman A, Egger S, Sitas F, Nair-Shalliker V. Obesity, physical activity and cancer risks: Results from the Cancer, Lifestyle and Evaluation of Risk Study (CLEAR). *Cancer Epidemiol* 2017;47:56–63.
3. Nair-Shalliker V, Yap S, Nunez C, Egger S, Rodger J, Patel MI, O'Connell DL, Sitas F, Armstrong BK, Smith DP. Adult body size, sexual history and adolescent sexual development, may predict risk of developing prostate cancer: Results from the New South Wales Lifestyle and Evaluation of Risk Study (CLEAR). *Int J Cancer* 2017;140:565–74.
4. Bashir MN. Epidemiology of prostate cancer. *Asian Pacific J Cancer Prev* 2015;16:5137–41.
5. Mandair D, Rossi RE, Pericleous M, Whyand T, Caplin ME. Prostate cancer and the influence of dietary factors and supplements: a systematic review. *Nutr Metab (Lond)* 2014;11:30.
6. NCEP -ATPIII. Third Report of the National Cholesterol Education Program (NCEP) Expert Panel on Detection, Evaluation, and Treatment of High Blood Cholesterol in Adults (Adult Treatment Panel III) final report. *Communication* 2002;106:3143–421.
7. Gacci M, Russo GI, De Nunzio C, Sebastianelli A, Salvi M, Vignozzi L, Tubaro A, Morgia G, Serni S. Meta-analysis of metabolic syndrome and prostate cancer. *Prostate Cancer Prostatic Dis* 2017;1–10.
8. Chinnadurai G. Transcriptional regulation by C-terminal binding proteins. *Int J Biochem Cell Biol* 2007;39:1593–607.
9. Moiola CP, Luca P De, Zalazar F, Cotignola J, Rodríguez-Seguí SA, Gardner K, Meiss R, Vallecorsa P, Pignataro O, Mazza O, Vazquez ES, De Siervi A. Prostate tumor growth is impaired by CtBP1 depletion in high-fat diet-fed mice. *Clin Cancer Res* 2014;20:4086–95.
10. De Luca P, Dalton GN, Scalise GD, Moiola CP, Porretti J, Massillo C, Kordon E,

Gardner K, Zalazar F, Flumian C, Todaro L, Vazquez ES, et al. CtBP1 associates metabolic syndrome and breast carcinogenesis targeting multiple miRNAs. *Oncotarget* 2016;7:18798–811.

11. Porretti J, Dalton GN, Massillo C, Scalise GD, Farré PL, Elble R, Gerez EN, Accialini P, Cabanillas AM, Gardner K, De Luca P, De Siervi A. CLCA2 epigenetic regulation by CTBP1, HDACs, ZEB1, EP300 and miR-196b-5p impacts prostate cancer cell adhesion and EMT in metabolic syndrome disease. *Int J Cancer* 2018;
12. Ellem SJ, Risbridger GP. Aromatase and regulating the estrogen: Androgen ratio in the prostate gland. In: Journal of Steroid Biochemistry and Molecular Biology. 2010. 246–51.
13. Liehr JG. Is estradiol a genotoxic mutagenic carcinogen? *Endocr Rev* 2000;21:40–54.
14. Ellem SJ, Risbridger GP. The dual, opposing roles of estrogen in the prostate. In: Annals of the New York Academy of Sciences. 2009. 174–86.
15. Ellem SJ, Schmitt JF, Pedersen JS, Frydenberg M, Risbridger GP. Local Aromatase Expression in Human Prostate Is Altered in Malignancy. *J Clin Endocrinol Metab* 2004;89:2434–41.
16. Bulun SE, Lin Z, Imir G, Amin S, Demura M, Yilmaz B, Martin R, Utsunomiya H, Thung S, Gurates B, Tamura M, Langoi D, et al. Regulation of aromatase expression in estrogen-responsive breast and uterine disease: from bench to treatment. *Pharmacol Rev* 2005;57:359–83.
17. Bulun SE, Simpson ER. Breast cancer and expression of aromatase in breast adipose tissue. *Trends Endocrinol Metab* 1994;5:113–20.
18. Micucci C, Valli D, Matacchione G, Catalano A. Current perspectives between metabolic syndrome and cancer. *Oncotarget* 2016;7:38959–72.
19. Iyengar NM, Hudis CA, Dannenberg AJ. Obesity and Cancer: Local and Systemic Mechanisms. *Annu Rev Med* 2015;66:297–309.
20. Kiwata JL, Dorff TB, Schroeder ET, Gross ME, Dieli-Conwright CM. A review of clinical effects associated with metabolic syndrome and exercise in prostate cancer patients. *Prostate Cancer Prostatic Dis.*2016;19:323–32.

21. Thalmann GN, Anezinis PE, Chang SM, Zhau HE, Kim EE, Hopwood VL, Pathak S, von Eschenbach AC, Chung LKW. Androgen-independent cancer progression and bone metastasis in the LNCaP model of human prostate cancer. *Cancer Res* 1994;54:2577–81.

22. To SQ, Simpson ER, Knower KC, Clyne CD. Involvement of early growth response factors in TNF??-induced aromatase expression in breast adipose. *Breast Cancer Res Treat* 2013;138:193–203.

23. To SQ, Knower KC, Cheung V, Simpson ER, Clyne CD. Transcriptional control of local estrogen formation by aromatase in the breast. *J. Steroid Biochem. Mol. Biol.*2015;145:179–86.

24. Llorens MC, Lorenzatti G, Cavallo NL, Vaglienti M V., Perrone AP, Carenbauer AL, Darling DS, Cabanillas AM. Phosphorylation Regulates Functions of ZEB1 Transcription Factor. *J Cell Physiol* 2016;231:2205–17.

25. De Siervi A, De Luca P, Byun JS, Di LJ, Fufa T, Haggerty CM, Vazquez E, Moiola C, Longo DL, Gardner K. Transcriptional autoregulation by BRCA1. *Cancer Res* 2010;70:532–42.

26. Smith JL, Freebern WJ, Collins I, De Siervi A, Montano I, Haggerty CM, McNutt MC, Butscher WG, Dzekunova I, Petersen DW, Kawasaki E, Merchant JL, et al. Kinetic profiles of p300 occupancy in vivo predict common features of promoter structure and coactivator recruitment. *Proc Natl Acad Sci U S A* 2004;

27. De Siervi A, De Luca P, Moiola C, Gueron G, Tongbai R, Chandramouli GVR, Haggerty C, Dzekunova I, Petersen D, Kawasaki E, Whoon JK, Camphausen K, et al. Identification of new Rel/NF??B regulatory networks by focused genome location analysis. *Cell Cycle* 2009;

28. De Luca P, Vazquez ES, Moiola CP, Zalazar F, Cotignola J, Gueron G, Gardner K, De Siervi A. BRCA1 loss induces GADD153-mediated doxorubicin resistance in prostate cancer. *Mol Cancer Res* 2011;9:1078–90.

29. Irusta G, Parborell F, Peluffo M, Manna PR, Gonzalez-Calvar SI, Calandra R, Stocco DM, Tesone M. Steroidogenic acute regulatory protein in ovarian follicles of

gonadotropin-stimulated rats is regulated by a gonadotropin-releasing hormone agonist. *Biol Reprod* 2003;68:1577–83.

30. Saragüeta P, Krimer ARD, Charreau EH, Tesone M. Insulin regulation of steroidogenic activity in rat culture luteal cells. *J Steroid Biochem* 1989;32:393–7.
31. Vona-Davis L, Howard-McNatt M, Rose DP. Adiposity, type 2 diabetes and the metabolic syndrome in breast cancer. *Obes Rev* 2007;8:395–408.
32. Guaita-Esteruelas S, Gum?? J, Masana L, Borr??s J. The peritumoural adipose tissue microenvironment and cancer. The roles of fatty acid binding protein 4 and fatty acid binding protein 5. *Mol. Cell. Endocrinol.*2016;
33. Toren P, Venkateswaran V. Periprostatic adipose tissue and prostate cancer progression: New insights into the tumor microenvironment. *Clin. Genitourin. Cancer*2014;12:21–6.
34. Cinti S, Mitchell G, Barbatelli G, Murano I, Ceresi E, Faloia E, Wang S, Fortier M, Greenberg AS, Obin MS. Adipocyte death defines macrophage localization and function in adipose tissue of obese mice and humans. *J Lipid Res* 2005;46:2347–55.
35. Carruba G. Estrogens and mechanisms of prostate cancer progression. In: Annals of the New York Academy of Sciences. 2006. 201–17.
36. Nieman KM, Kenny HA, Penicka C V., Ladanyi A, Buell-Gutbrod R, Zillhardt MR, Romero IL, Carey MS, Mills GB, Hotamisligil GS, Yamada SD, Peter ME, et al. Adipocytes promote ovarian cancer metastasis and provide energy for rapid tumor growth. *Nat Med* 2011;17:1498–503.
37. Wang F, Gao S, Chen F, Fu Z, Yin H, Lu X, Yu J, Lu C. Mammary fat of breast cancer: Gene expression profiling and functional characterization. *PLoS One* 2014;9.
38. Shafat MS, Oellerich T, Mohr S, Robinson SD, Edwards DR, Marlein CR, Piddock RE, Fenech M, Zaitseva L, Abdul-Aziz A, Turner J, Watkins JA, et al. Leukemic blasts program bone marrow adipocytes to generate a protumoral microenvironment. *Blood* 2017;129:1320–32.

FIGURE TO LEGENDS

Figure 1. CTBP1 represses *CYP19A1* transcription in PC3 cell line. *A) CYP19A1* mRNA levels in PCa cell lines measured by RT-qPCR. *B) CYP19A1* and *CTBP1* gene expression levels by RT-qPCR from CTBP1 overexpressed PC3 cells. *C)* CYP19A1, CTBP1, and β-Actin protein levels from CTBP1 overexpressed PC3 cells by WB. Quantification and normalization to β-Actin protein levels and pcDNA3 are shown under each band. One representative experiment from two biologic replicates is shown. *D) CYP19A1* and *CTBP1* gene expression levels by RT-qPCR from PC3.pGIPZ and PC3.shCTBP1 stable cell lines. Bars indicate mean and SD of two independent experiments. *E)* Plasmids with different length of the I.4 (PG1 to PG10) or PII *CYP19A1* promoters were co-transfected with CTBP1 or control (pcDNA3) plasmids in PC3 cells, and Luciferase activity was determined. Bars indicate mean and SD of two independent experiments with three replicates. *F)* ChIP-qPCR using CTBP1 or nonspecific (Gal4) antibodies and primers located at -0.5 Kb and 0 Kb upstream of the TSS of *CYP19A1* or -0.2 Kb upstream of the *HBB* TSS promoter region. Fold enrichment was calculated normalizing data to input and Gal4. Bars represent the average and SD from one representative experiment.

Figure 2. EP300 , CTBP1, ER-β and estradiol regulates *CYP19A1* transcription. *A)* PC3 cells were co-transfected with the I.4 *CYP19A1* promoter reporter (-1004/+14) (PG1-luc) and pcDNA3, CTBP1, EP300, E2F1, STAT3, RELA, SF1 or ZEB1 expression plasmids and

Luciferase activity was determined. Mean of two independent experiments with three replicates and SD is plotted. *B)* PC3 cells were co-transfected with PG1-luc or PII (-516/+16) (PII-luc) *CYP19A1* promoter reporters and CTBP1 or control (pcDNA3) plasmids *plus* EP300 and Luciferase activity was determined. Mean of two independent experiments with three replicates and SD is plotted. *C)* ChIP-qPCR using EP300 or nonspecific (Gal4) antibodies and primers located at -0.5 Kb and 0 Kb upstream of the TSS of *CYP19A1* or -0.2 Kb upstream of the *HBB* TSS promoter region. Fold enrichment was calculated normalizing data to input and Gal4. Bars represent the average and SD from one representative experiment. *D)* mRNA *CYP19A1* levels measured by RT-qPCR from PC3 cells after ER-β plasmid transfection and exposed to estradiol (E_2) for 96 h. Mean of two independent experiments and SD is plotted. *E)* PC3 cells were co-transfected with PG1-luc promoter reporter and pcDNA3, ER-α or ER-β expression plasmids. After 24 h, cells were exposed to estradiol or vehicle for 48 h and Luciferase activity was determined. Mean of two independent experiments with three replicates and SD is plotted. *F)* PC3 cells were co-transfected with PG1-luc or PII-luc promoter reporters and CTBP1 or control (pcDNA3) plasmids plus ER-β. After 24 h, cells were exposed to estradiol or vehicle for 48 h and Luciferase activity was determined. Mean of two independent experiments with three replicates and SD is plotted. *a)* CTBP1 E_2 0 vs CTBP1+ER-β E_2 1 µM. *b)* CTBP1 E_2 0 vs CTBP1+ER-β E_2 10 µM. *c)* pcDNA3 E_2 0 vs CTBP1+ER-β E_2 10 µM. *G)* PC3 cells were grown in RPMI without phenol red supplemented with charcoal-stripped 10% FBS. After 24 h, cells were exposed to estradiol or vehicle for 96 h. ChIP-qPCR using CTBP1, EP300 or nonspecific (Gal4) antibodies and primers located at -0.5 Kb and 0 Kb upstream of the TSS

of *CYP19A1* or -0.2 Kb upstream of the *HBB* TSS promoter region. Fold enrichment was calculated normalizing data to input and Gal4. Bars represent the average and SD from one representative experiment.

Figure 3. Estradiol modulates the viability and cell cycle progression of a panel of PCa cell lines. *A)* PCa cells were grown in RPMI without phenol red supplemented with charcoal-stripped 10% FBS. After 24 h, cells were exposed to estradiol or vehicle for 96 h and cell viability was determined by MTS assay. Mean of three replicates and SD is plotted. Data were normalized to E_2 0. *B)* PCa cells were grown in RPMI media without phenol red supplemented with charcoal-stripped 10% or 1 % FBS. After 24 h, cells were exposed to estradiol or vehicle for 96 h and cell cycle analysis was performed. The figure shows the percentage of cells in G0/G1, S, and G2/M phases from two biological replicates. *C) CYP19A1* and *CTBP1* RT-qPCR from xenografts with CTBP1 depleted (PC3.shCTBP1) or control (PC3.pGIPZ) expression generated in HFD or CD fed NSG mice. *D)* Intratumor estradiol levels from xenografts with CTBP1 depleted (PC3.shCTBP1) or control (PC3.pGIPZ) expression generated in HFD fed NSG mice were measured by RIA. Boxes represent the interquartile range, the horizontal line within each box represents the median, and the upper and lower whiskers represent the SD of one experiment (N=6).

Figure 4. HFD increases TRAMP-C1 allograft tumor growth and serum estradiol levels while induces *Ctbp1*, *Fabp4* and *IL-6* gene expression. *A)* TRAMP-C1 cells were grown in DMEM without phenol red supplemented with charcoal-stripped 10% FBS. After 24 h, cells

were exposed to estradiol or vehicle for 96 h and cell viability was determined by MTS assay. Mean of three replicates and SD is plotted. Data were normalized to E_2 0. *B)* Tumor growth from CD or HFD C57BL/6J mice inoculated with TRAMP-C1 cell line. Curves indicate media and SD values of one representative experiment (n=6). *C)* Serum estradiol levels from CD or HFD fed C57BL/6J mice were measured by RIA. Boxes represent the interquartile range, the horizontal line within each box represents the median, and the upper and lower whiskers represent the standard deviation of one independent experiment (n=6). *D) Ctbp1* and *Ctbp2* RT-qPCR from HFD or CD allografts samples. Data were normalized to *ACTB* and control. *E)* CTBP1 IHC from tumor allografts developed in CD or HFD fed C57BL/6J mice. Magnification 100x and 400x. *F)* RT-qPCR from HFD or CD allografts samples using specific primers for the indicated genes. Data were normalized to *ACTB* and control.

Figure 5. MeS induces alterations of gWAT which induces TRAMP-C1 cell proliferation and *Ctbp1*/*IL6* gene expression.

A) Mesenteric and gonadal/epididymal fat depots weights from CD or HFD fed C57BL/6J mice. *B)* H&E of gWAT from CD or HFD fed C57BL/6J mice. Arrows indicate representative adipocytes. Box plot represent adipocyte size quantitation calculated by Image J. *C)* H&E of gWAT from CD of HFD fed C57BL/6J mice showing in high magnification CLS. Magnification 100 and 400x. Bars represent media and SD of the CLS counts *per* mm^2. *D-F)* RT-qPCR from gWAT samples obtained from CD or HFD fed C57BL/6J mice using specific primers for the indicated genes. Data were normalized to *ACTB* and control. *G)* TRAMP-C1

cancer cells were counted after co-cultured with gWAT obtained from CD of HFD C57BL/6J fed mice for 48 h. As control, TRAMP-C1 cells were incubated in DMEM complete media without the addition of gWAT. Data were normalized to control and represent mean and SD of three independent experiments with six replicates. *H)* RT-qPCR from TRAMP-C1 cells obtained from the co-culture using specific primers for the indicated genes. Data were normalized to *ACTB* and control and represent mean and SD of two independent experiments with three replicates. *I)* RT-qPCR from gWAT obtained from the co-culture using specific primers for the indicated genes. Data were normalized to *ACTB* and control and represent the mean and SD of two independent experiments with three replicates. *J) IL-6* production was measured in supernatant from the co-cultures. Bars represent average and SD of three independent experiments with three replicates.

Figure 6. Hypothetical model: *1)* CTBP1 protein assembles with EP300 to I.4 and PII *CYP19A1* proximal promoter regions and represses its transcription in Androgen insensitive (AI) PCa cells. *2)* MeS induces adipogenesis, which increases amount of AT, and AT inflammation resulting in IL-6 and serum estradiol concentration induction. *3)* Estradiol from this conversion, through ER-β, releases CTBP1 from *CYP19A1* promoters, induces its transcription and decreases AI PCa cell proliferation. *4)* Estradiol increases Androgen sensitive (AS) PCa cell proliferation. In addition, MeS transcriptionally activates endogen *Ctbp1*, *Fabp4* and *IL6* in AS PCa tumors modulating PCa growth.

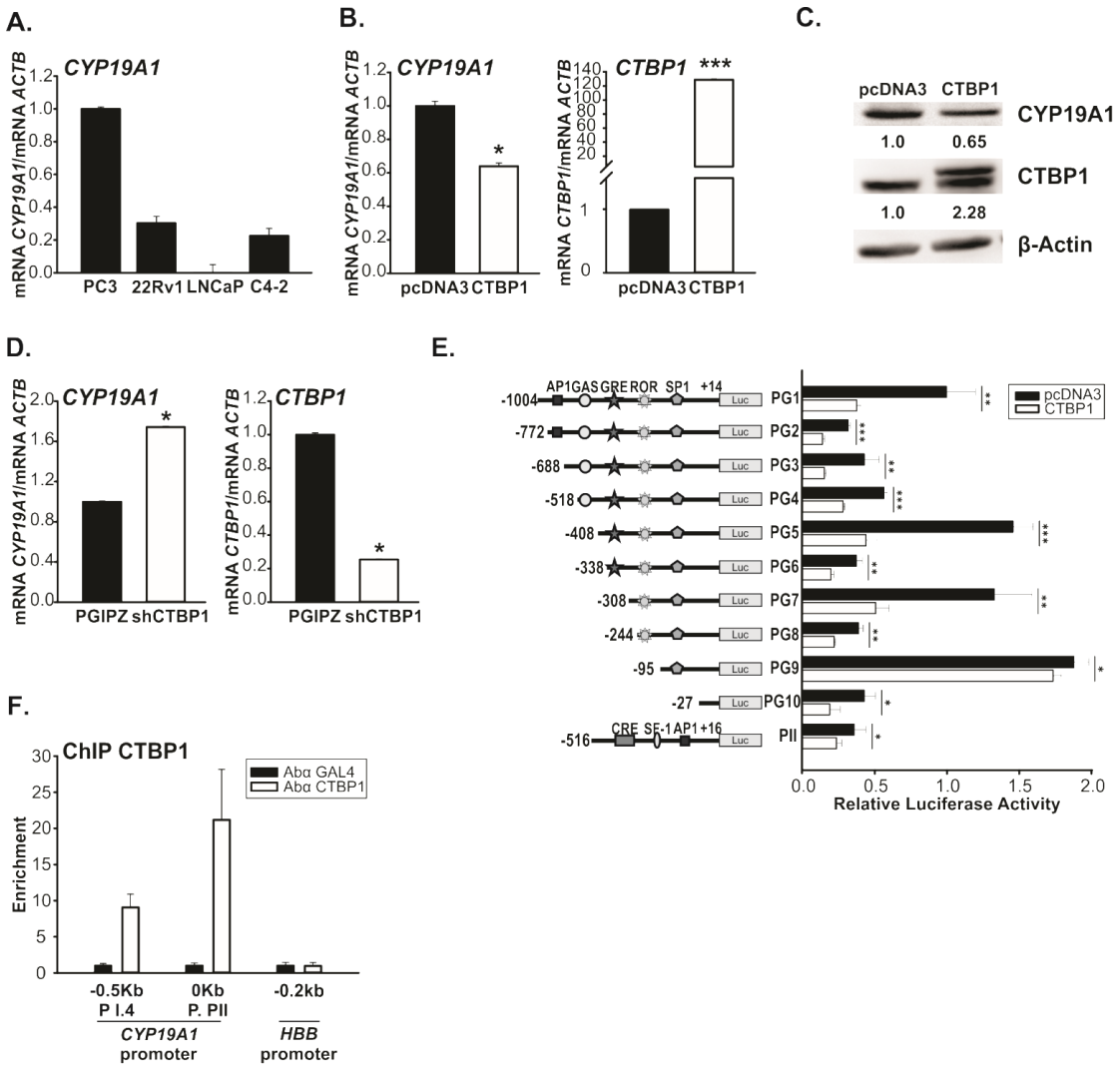

Figure 1.

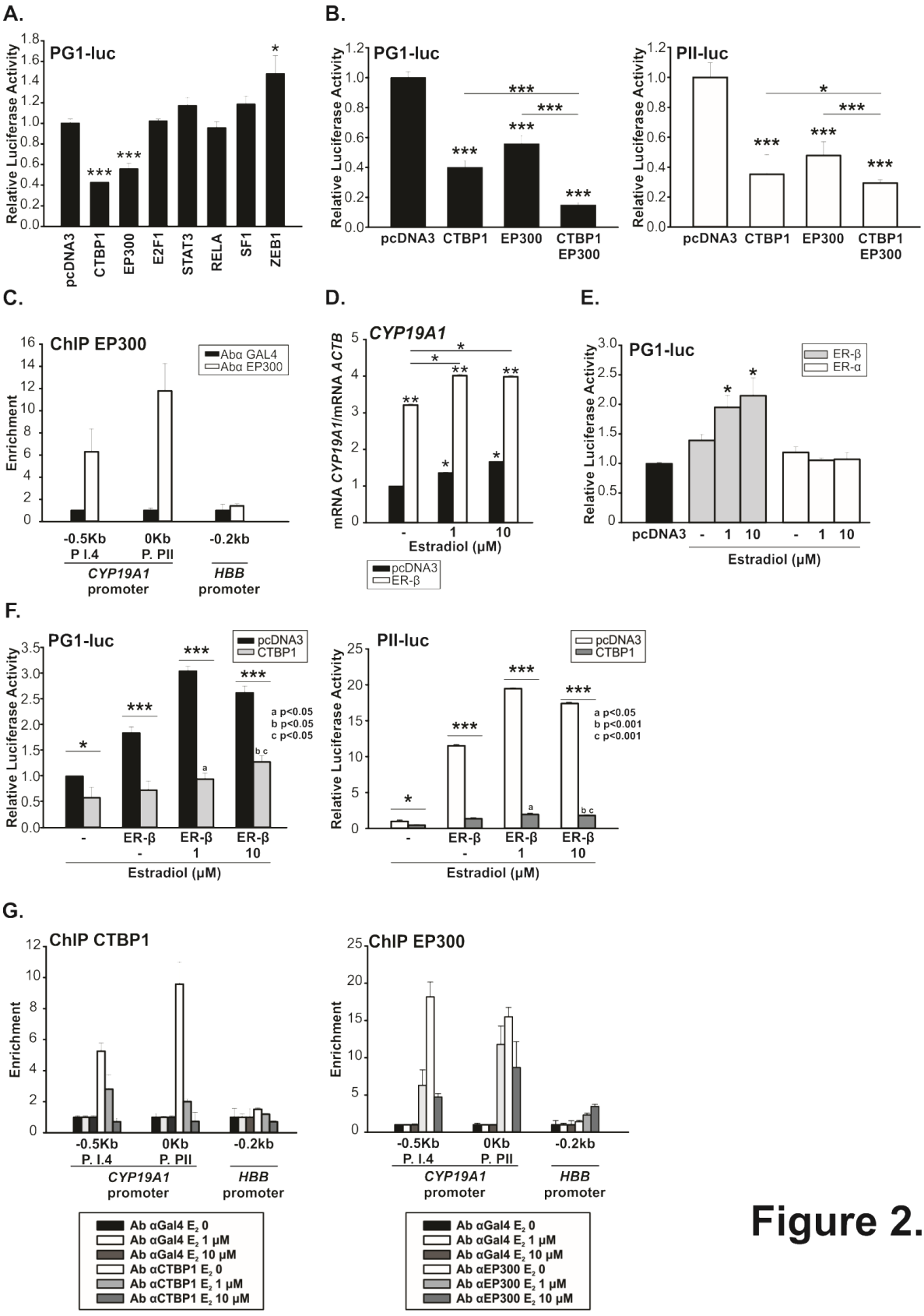

Figure 2.

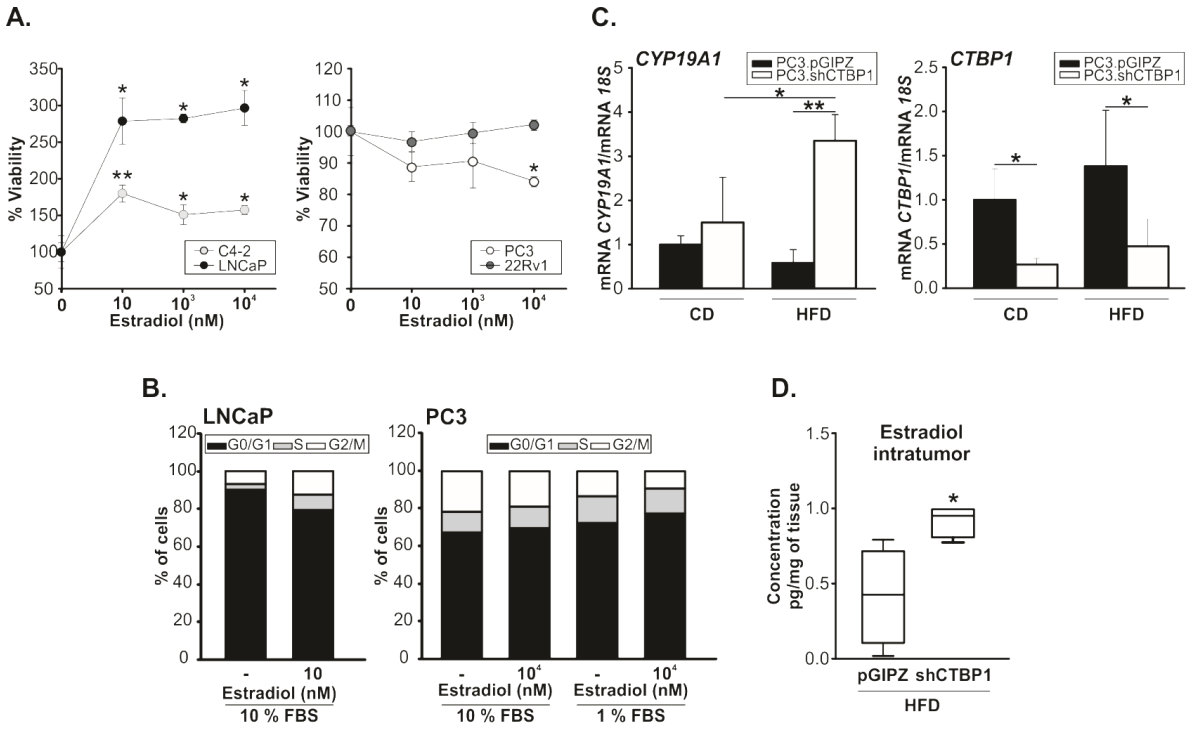

Figure 3.

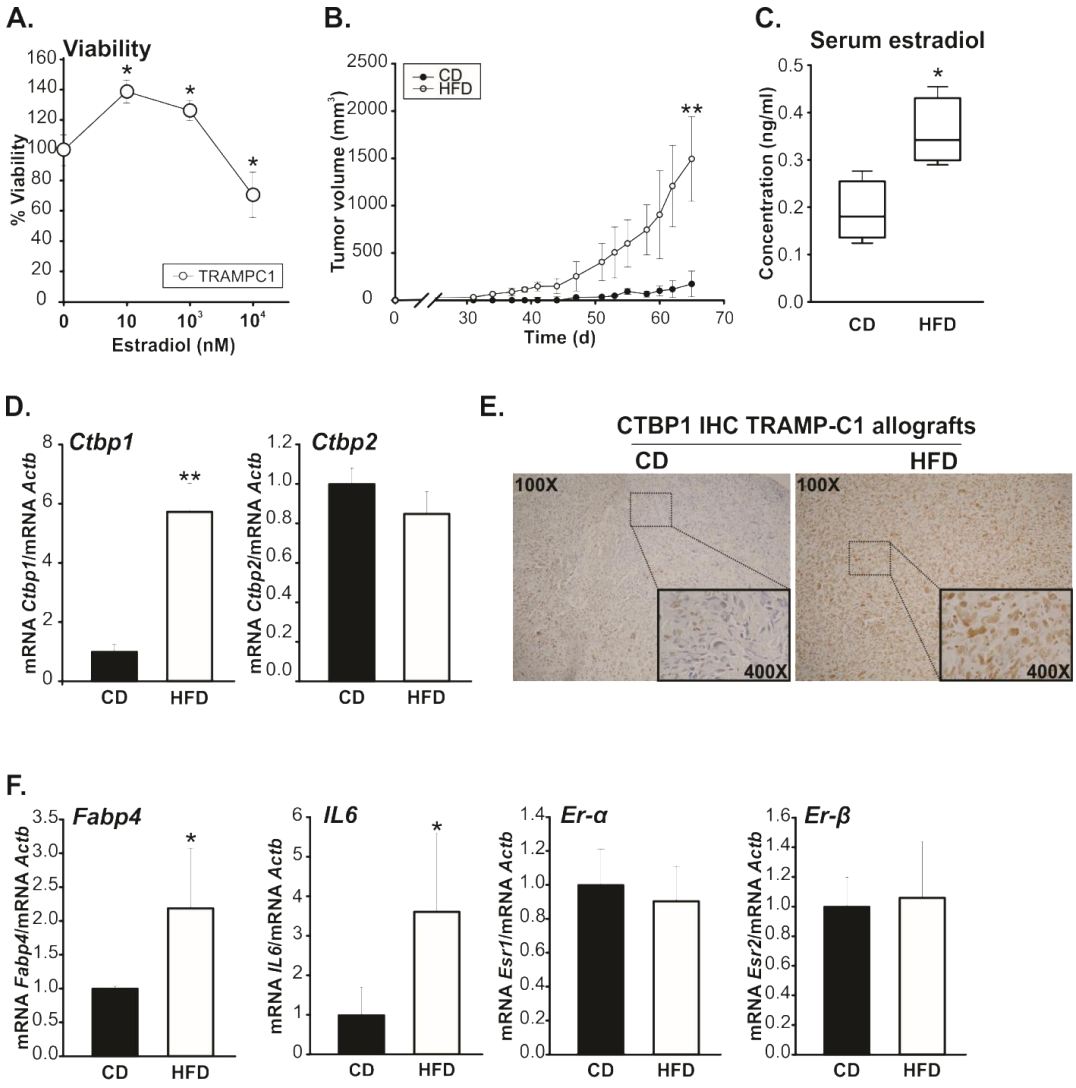

Figure 4.

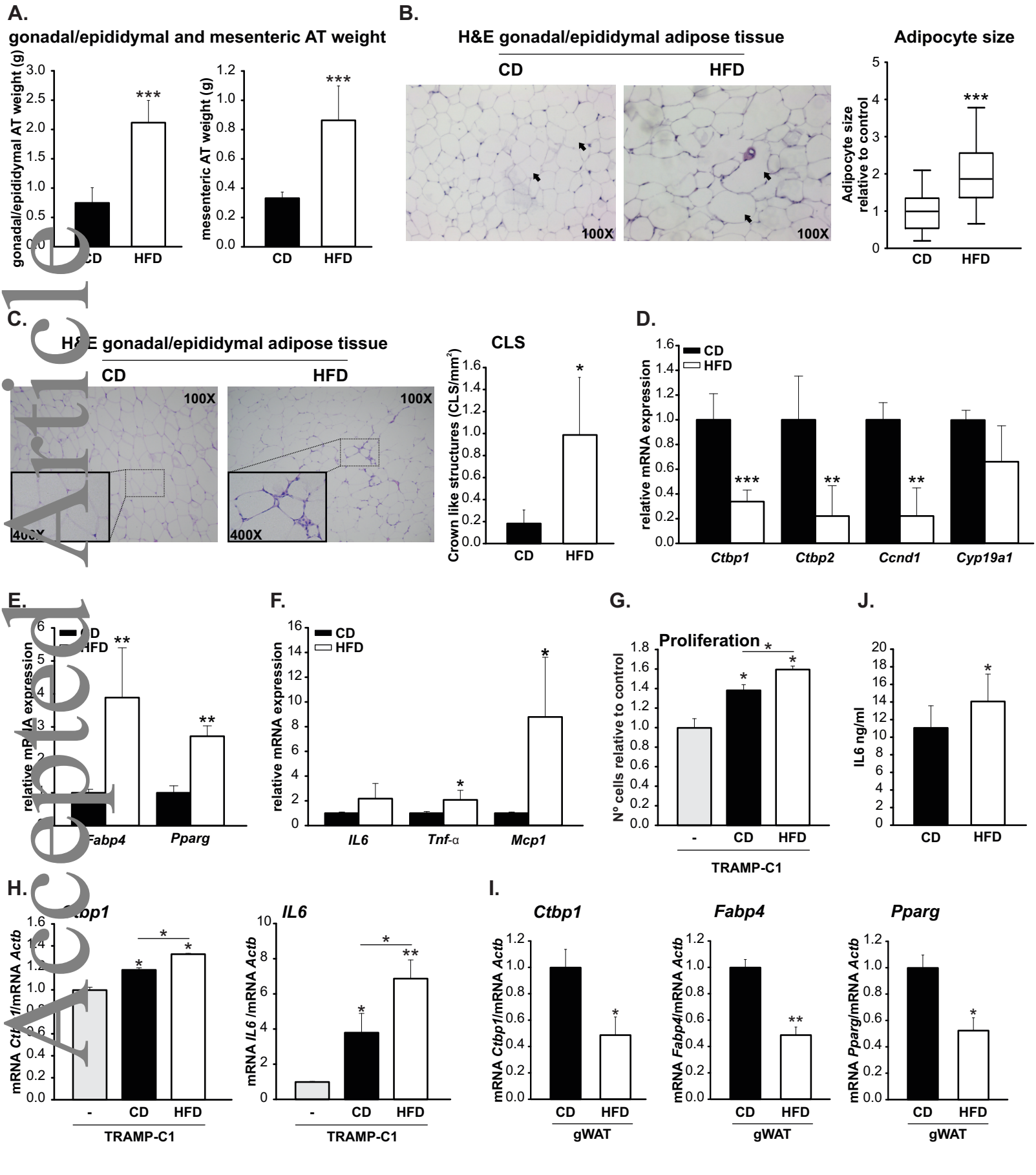

Figure 5.